THE JOURNAL OF PHYSICAL CHEMISTRY B

Article

pubs.acs.org/JPCB

Ion-Cage Interpretation for the Structural and Dynamic Changes of Ionic Liquids under an External Electric Field

Rui Shi and Yanting Wang*

State Key Laboratory of Theoretical Physics, Institute of Theoretical Physics, Chinese Academy of Sciences, 55 East Zhongguancun Road, P.O. Box 2735, Beijing 100190, China

Supporting Information

ABSTRACT: In many applications, ionic liquids (ILs) work in a nonequilibrium steady state driven by an external electric field. However, how the electric field changes the structure and dynamics of ILs and its underlying mechanism still remain poorly understood. In this paper, coarse-grained molecular dynamics simulations were performed to investigate the structure and dynamics of 1-ethyl-3-methylimidazolium nitrate ([EMIm][NO_3]) under a static electric field. The ion cage structure was found to play an essential role in determining the structural and dynamic properties of the IL system. With a weak or moderate electric field (0−10^7 V/m), the external electric field is too weak to modify the ion cage structure in an influential way and thus the changes of structural and dynamic properties are negligible. With a strong electric field (10^7−10^9 V/m) applied, ion cages expand and deform apparently, leading to the increase of ion mobility and self-diffusion coefficient with electric field, and the self-diffusion of ions along the electric field becomes faster than the other two directions due to the anisotropic deformation of ion cages. In addition, the Einstein relation connecting diffusion and mobility breaks down at strong electric fields, and it also breaks down for a single ion species even at moderate electric fields (linear-response region).

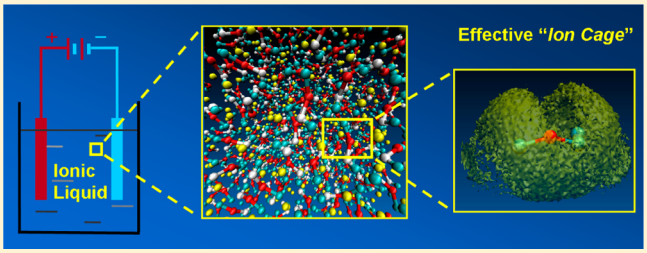

1. INTRODUCTION

Ionic liquids (ILs) have many unique properties such as low volatility, tunable solubility, good thermal and chemical stabilities, and conductivity, which make ILs very promising in industry.[1−4] In many applications, especially when ILs are used as electrolytes in electrochemical devices, such as lithium secondary batteries,[5,6] fuel cells,[5,7] electrospray,[8] and electrophoresis systems,[9] ILs work in a (nearly) nonequilibrium steady state driven by a static external electric field. In these applications, high ion transport is desired, but due to the relatively high viscosity of ILs, their slow ion mobility and diffusion are the major obstacles that limit the applications of ILs as electrolytes.[10] Therefore, great efforts have been made to investigate the dynamic properties of ILs. Nevertheless, previous studies have mainly focused on the equilibrium properties of ILs, whereas, from a theoretical perspective, the properties measured and calculated under equilibrium conditions may not be naturally applied to nonequilibrium states. Moreover, the theorems established for equilibrium states might fail in nonequilibrium states. Therefore, a deeper understanding of the structure and dynamics of ILs in nonequilibrium steady states is of great importance for the electrochemical applications of ILs.

Compared with the extensive studies on equilibrium properties of ILs in the past decade, investigation on nonequilibrium behavior of ILs is still in its infancy. Only a few experiments[11,12] and simulations[13−20] have been performed to study the structure and dynamics of ILs under an external electric field. Nuclear magnetic resonance (NMR) measurements have revealed the promotion of ion transport in ILs under a weak electric field. For example, Saito and co-workers[12] reported that the measured mobilities of several neat ILs jump abruptly at a threshold electric field around 100 V/m. In contrast, Hayamizu et al.[11] found a gradual increase of the diffusion coefficient with an increasing electric field from 0 to 300 V/m. The two controversial experiments raised two questions: (1) As the electric field increases, do the transport properties increase gradually or abruptly? (2) What is the microscopic mechanism that can explain the structural and dynamic changes of ILs when an external electric field is applied?

Recently, the interfacial structures of ILs on charged electrodes have been widely studied. Under an electric field between two electrodes, ILs form an electric double layer with the interfacial layering of ions extending into the bulk for several nanometers, which has been reported in many experiments[21,22] and simulations.[23−38] However, those studies have focused on the equilibrium interfacial structure of ILs under an external electric field, leaving behind a profound understanding of the nonequilibrium structure and dynamics of ILs. In fact, when ILs are used as electrolytes in electrochemical devices, they usually work in a nonequilibrium state, in which

Received: November 7, 2012
Revised: April 4, 2013
Published: April 4, 2013

   dx.doi.org/10.1021/jp311017r | J. Phys. Chem. B 2013, 117, 5102−5112

the bulk ions are driven to drift by an external electric field, leading to a net ionic current.

Just as a powerful tool for studying equilibrium properties of ILs, in recent years, molecular dynamics (MD) simulations have also been employed to investigate their nonequilibrium properties. English et al.[15,16] studied the effect of strong electromagnetic field on the structure and dynamics of ILs as well as their water mixtures. The nonequilibrium MD simulations were also used to study the heterogeneous structure,[19,20] conductivity,[17] electrospray,[13,14] polarization relaxation,[35] and hydrophilicity[18] of ILs under a strong static electric field. In agreement with experiments, dynamic changes of ILs under an external electric field were observed in those MD simulations. However, a large gap between the strengths of the electric fields applied in experiments and simulations disallows a straightforward comparison of simulation results with experiments. In experiments, weak electric fields ($E < 10^6$ V/m) are usually applied to avoid decomposition of ILs. In contrast, MD simulations are always performed at strong electric fields ($E > 10^7$V/m) to make the ion drift observable during the simulation time, which is typically tens of nanoseconds. Moreover, no microscopic mechanisms have been proposed to clearly explain the dynamic changes of ILs under an external electric field. Therefore, a unified microscopic mechanism is greatly desired to provide consistent explanations for both experiments and simulations.

The effective concept of *cage* was proposed a long time ago to understand the microscopic structure and dynamics of liquids beyond the continuous hydrodynamic model.[39] From the statistical point of view, on ensemble average, one molecule can be considered as surrounded by an effective "cage" composed of several neighboring molecules in the first coordination shell. This central molecule thermally vibrates inside the cage and frequently escapes from the cage and diffuses.[40−43] The above concept of cage is also applicable to IL systems.[44−53] Since ILs are composed solely of ions, an *ion cage* forms with a central ion encapsulated by its neighboring counterions in the first coordination shell, as a result of the local charge ordering in ILs.[47,54−57] Due to the very strong intrinsic electrostatic interactions in ILs,[58] ions are usually trapped in their cages for a long time, which results in the slow dynamics of ILs. Systematic investigation of the ion cage structure can provide new insight into the structural and dynamic properties of nonequilibrium IL systems.

In the present work, MD simulations with the effective force coarse-graining (EF-CG) model[59,60] of the 1-ethyl-3-methylimidazolium nitrate ([EMIm][NO_3]) IL have been conducted to study its structure and dynamics under a static electric field ranging widely from 0 to 10^9 V/m, and a microscopic mechanism has been suggested on the basis of the analysis of simulation results from the *ion cage* perspective. We found that, at weak or moderate electric fields ($0 < E \leq 10^7$ V/m), the dynamic properties and the underlying ion cage structure both show no measurable changes. When a strong electric field (10^7 V/m $< E \leq 10^9$ V/m) is applied, the ion cage expands, which lowers the energy barrier of the effective cage potential well and hence boosts the mobility and self-diffusion of ions. Besides, the strong electric field deforms the ion cage to be anisotropic, so the effective cage potential well and thus the self-diffusion also become anisotropic. In addition, the Einstein relation connecting diffusion and mobility breaks down at strong electric fields and it also breaks down for a single ion species even at moderate electric fields (linear-response region).

2. SIMULATION AND ANALYSIS METHODS

2.1. Simulation Methods and Procedure. At weak and moderate electric fields, drift velocities of ions are very small, so a long time simulation is necessary to allow them to be more detectable. Since the EF-CG MD simulation[60] has an accelerated dynamics compared with corresponding all-atom MD simulations, the EF-CG model of the [EMIm][NO_3] IL[59] was used to perform the MD simulations. The atomistic molecular structure and the EG-CG model of [EMIm][NO_3] are shown in Figure 1. In the CG strategy, the nitrate anion is

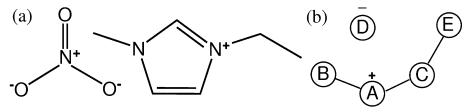

Figure 1. Atomistic molecular structure (a) and coarse-grained model (b) of [EMIm][NO_3].

coarse-grained as CG site D, the imidazolium ring as site A, the methyl group attached to the ring as site B, and the methylene and methyl groups on the alkyl chain as sites C and E, respectively.

Although only one IL ([EMIm][NO3]) was studied in this work, we believe that the ion cage concept and the microscopic mechanism of an IL responding to an external electric field are applicable to other ILs, despite their differences in chemical details, for the following reasons: (1) the ion cage concept is based on the charge ordering which has been observed in various ILs; (2) regardless of chemical details, it is the competition between the internal and external fields, which exists in all ILs, that determines the structural and dynamic changes of ILs under an external field.

The [EMIm][NO_3] system with 512 ion pairs in a periodic cubic simulation box with a side length of about 50 Å has been simulated with a static electric field E ranging from 0 to 10^9 V/m applied along the X direction. In the rest of the paper, we refer the term "weak electric field" to the range $0 < E < 10^6$ V/m, "moderate" to 10^6 V/m $\leq E \leq 10^7$ V/m, and "strong" to 10^7 V/m $< E \leq 10^9$ V/m. The long-range electrostatic interactions were treated by the Ewald sum. A cutoff distance of 14 Å was applied for both the van der Waals and the real part of the electrostatic interactions. All the simulations were performed by using the DL_POLY program[61] with a time step of 4 fs.

An equilibrated initial configuration was taken from our previous simulation.[59] A constant *NPT* nonequilibrium MD simulation at $T = 400$ K and $P = 1$ atm was performed for 4 ns to allow the system to reach its steady state as well as to determine the average system size. For the case of weak electric fields, a constant *NVT* production run for 20 ns was followed to collect data. For the case of moderate or strong electric fields, for each E, a constant *NVT* run at $T = 2000$ K was then performed for 10 ns to generate 20 random initial configurations by evenly sampling along this 10 ns trajectory. Beginning from these random initial configurations, 20 independent constant *NVT* production runs at $T = 400$ K were carried out. The duration of these runs was 4 ns for each moderate electric field and 2 ns for each strong electric field. For comparison, an equilibrium constant *NVT* run was also performed for 40 ns without an electric field at $T = 400$ K. All simulation data were evenly sampled every 1000 steps from each trajectory. In order to calculate the conductivity by the Green−Kubo relation, another equilibrium constant *NVT* run

dx.doi.org/10.1021/jp311017r | J. Phys. Chem. B 2013, 117, 5102−5112

was conducted without an electric field for 4 ns with the velocity recorded every five steps.

To see if a 2−4 ns CG trajectory is sufficient for studying the structure and dynamics of [EMIm][NO_3], we checked the convergence of potential energy and self-diffusion coefficient of the IL system, as shown in section A in the Supporting Information. Moreover, an ensemble of many independent short trajectories can explore the phase space more adequately than a single long trajectory. In all MD simulations, the temperature was kept constant by using the Nosé−Hoover thermostat.[62,63] In principle, the validity of applying a thermostat developed for equilibrium conditions to a nonequilibrium MD simulation is questionable. In practice, we may still use it if the error is acceptable. A detailed discussion of the validity of thermostats in nonequilibrium MD simulations is given in section B in the Supporting Information.

2.2. Calculation of Drift Velocity. Since the drift motion of ions is usually submerged in the noisy self-diffusion at the molecular level, the determination of the drift velocity or, equivalently, the mobility by MD simulation is still very challenging. For example, the drift velocity of the [EMIm][BF_4] IL is about 10^{-7} m/s at an electric field of E = 100 V/m, much smaller than its thermal velocity of 190 m/s at T = 298 K (see section C in the Supporting Information for details). Consequently, the small drift motion is entirely submerged in the large thermal motion at the molecular level. Only when a very strong electric field is applied can the drift velocity be directly calculated from the average ion velocity.[14] This is the reason why most of the nonequilibrium simulations only focused on the behavior of ILs at strong external electric fields. This problem is quite general in the nonequilibrium MD simulations of various electrolytes including ILs. Near equilibrium, the Einstein relation

$$D = uk_BT/ze \tag{1}$$

can be used to calculate the mobility u from the diffusion coefficient D, where T is the temperature and ze is the charge of the ion. However, since the Einstein relation was found to break down when the system is far from equilibrium,[64] as also demonstrated by this work (see section 5.2), this method fails to obtain the mobility under an external electric field. Therefore, a new method to calculate the drift velocity or, equivalently, the mobility is desired.

In the present paper, an approach previously developed for theoretical and numerical calculations[65,66] has been introduced to calculate the drift velocity in MD simulations. In simulation, the spontaneous displacement of ion i along the direction of the external field in a time interval Δt at a time t_j can be decomposed into a random diffusive term and a directional drift term:

$$\Delta r_i(t_j) = \Delta r_i^{\text{diffusion}}(t_j) + \Delta r_i^{\text{drift}}(t_j) \tag{2}$$

Because the diffusive motion is random walk in all directions and has a spectrum of white noise, for an infinite number of spontaneous displacements, we have

$$\lim_{M\to\infty} \frac{1}{M} \sum_{j=1}^{M} \Delta r_i^{\text{diffusion}}(t_j) = 0 \tag{3}$$

where M is the number of time intervals. Therefore, the drift velocity can be approximately calculated from a finite length of trajectory by using the equation

$$v_{\text{traj}} = \frac{1}{N\cdot M} \sum_{i=1}^{N} \sum_{j=1}^{M} \frac{\Delta r_i^{\text{drift}}(t_j)}{\Delta t} = \frac{1}{N\cdot M} \sum_{i=1}^{N} \sum_{j=1}^{M} \frac{\Delta r_i(t_j)}{\Delta t} \tag{4}$$

where N is the number of ions. In practice, we calculate a series of Δr with respect to different Δt and determine v_{traj} by linear fitting the curve of Δr versus Δt. If we replace the long time average by the ensemble average of many independent short trajectories, we estimate the ion drift velocity by

$$v_{\text{drift}} = \langle v_{\text{traj}} \rangle \tag{5}$$

where the brackets $\langle \cdots \rangle$ denote the ensemble average over all trajectories.

2.3. Quantification of Structural Properties. In the IL system, by assuming the ion position distribution $P(r)$ in the ion cage (r is the spontaneous deviation of the central ion from the center of mass of its ion cage) is independent of the momenta, cage positions, and directions, $P(r)$ can be computed from the simulation data and then fitted with a Boltzmann distribution in each direction as

$$P(r) = A\cdot\exp\left[-\frac{U(r)}{k_BT}\right] \tag{6}$$

where $U(r)$ is the effective cage potential, k_B is the Boltzmann constant, T is the temperature, and A is a normalization coefficient. In this way, we can determine the effective one-dimensional cage potential $U(r)$ that characterizes the strength of the effective cage potential well.

2.4. Quantification of Dynamic Properties. Besides the drift velocity, the cage dynamics describing the relaxation of ion cage structure was analyzed by using the continuous time correlation function (TCF)[46,67]

$$C_{\text{cage}}(t) = \frac{\langle p(0)P(t)\rangle}{\langle p\rangle} \tag{7}$$

where the population variable $p(t)$ is unity if one ion pair contacts at time t and zero otherwise. The survival index $P(t)$ is unity when the tagged ion pair remains in contact continuously until time t and zero otherwise. $\langle p\rangle$ denotes the average value of p. Here the two ions are regarded as being in contact if their distance is shorter than a cutoff of 7 Å, which is the first valley position of the cation−anion radial distribution function (see Figure 3a). By definition, a central ion only contacts with its neighboring counterions in its ion cage.

The mobility u, which quantifies the ability of ion movement in response to an external electric field, can be calculated by

$$u = v_{\text{drift}}/E \tag{8}$$

where v_{drift} is the drift velocity and E is the strength of the applied electric field. The diffusive motion of ions was characterized by the effective self-diffusion coefficient D_{eff} for each direction[65,66]

$$D_{\text{eff}} = \lim_{t\to\infty} \frac{\langle x^2(t)\rangle - \langle x(t)\rangle^2}{2t} \tag{9}$$

where $\langle x^2(t)\rangle$ is the mean-square displacement and $\langle x(t)\rangle$ is the drift movement of ions.

dx.doi.org/10.1021/jp311017r | J. Phys. Chem. B 2013, 117, 5102−5112

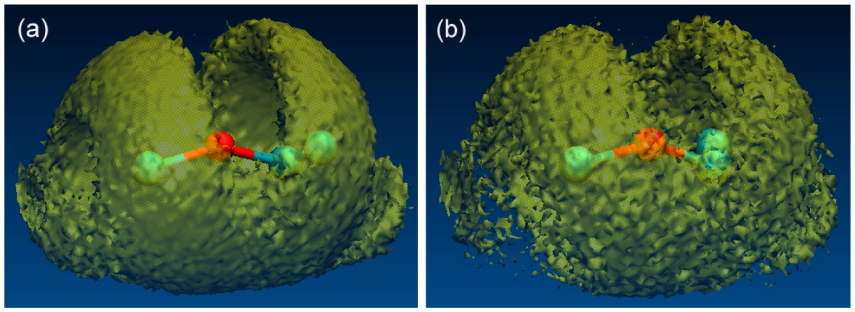

Figure 2. Spatial distribution of anions around a cation with an isosurface value of 0.009 $Å^{-3}$ in the absence (a) and presence (b) of an external electric field of 10^9 V/m. Red: site A in cation. Cyan: sites B, C, and E in cation.

3. STRUCTURAL CHANGES

3.1. Ion Cage Structure. Due to the very strong intrinsic electric field in ILs,[58] ions are always surrounded by several counterions. Figure 2 shows the spatial distributions of anions around a cation in the absence and presence of an external electric field of 10^9 V/m, respectively.

It can be seen that, regardless of the external electric field, the cation is almost encapsulated by anions in its first coordination shell, forming an ion cage structure. With a strong electric field applied, the spatial distribution of anions is more ragged and the anions have less probability to appear near CG sites B and E.

In order to further investigate the ion cage structure of [EMIm][NO_3], the center-of-mass radial distribution functions (RDFs) were calculated, as shown in Figure 3. The RDFs for weak and moderate electric fields (only $E = 10^6$ and 10^7 V/m are shown) overlap with each other. For all the electric fields applied, the oscillations of the cation−anion RDFs have an opposite phase compared with the cation−cation and anion−anion RDFs. This indicates that the local charge ordering in [EMIm][NO_3], commonly observed in ILs,[47,54−57] still remains under an external electric field. Both spatial and radial distribution functions agree with the fact that ions in ILs are surrounded by several counterions, forming an ion cage structure. Our calculations indicate that, in the [EMIm][NO_3] IL, each ion is surrounded by 6.1 ± 0.8 counterions.

Figure 3a shows the cation−anion RDFs at different electric fields. As the external electric field increases, the first peak of the cation−anion RDFs shifts to the left and its value becomes smaller, but the probability of ions appearing in the first minimum slightly increases. This phenomenon is known as the relaxation effect,[68] with which the central ion position distribution in its cage is biased. Parts b and c of Figure 3 show the cation−cation and anion−anion RDFs, respectively. The right shift of the first peak illustrates the slightly larger separation of ions with the same sign with increasing electric field, demonstrating a slight expansion of ion cage under a strong electric field. However, no expansion was observed at moderate electric fields, as indicated by the overlapped RDFs at $E = 10^6$ and 10^7 V/m. This result is consistent with the change of system density that apparently decreases with increasing strong electric fields but shows no obvious change under moderate electric fields (see section D in the Supporting Information).

3.2. Effective Cage Potential Well. Several studies[45,48,49] have suggested that, due to the strong ion−ion interactions in ILs, the ion cage plays an important role in determining the dynamic properties of ILs. One usually accepts the microscopic

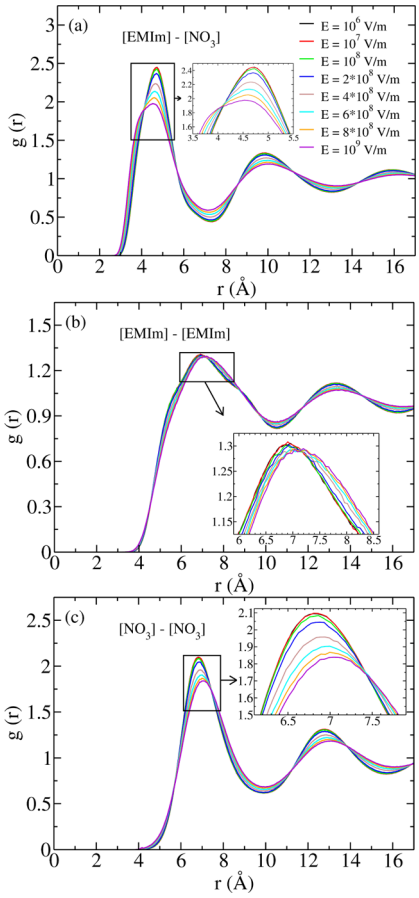

Figure 3. Radial distribution functions between the center of mass of cations and anions (a), cations and cations (b), and anions and anions (c), under different strengths of external electric fields. The insets show the enlarged images of the rectangular regions.

picture that an ion is trapped and thermally vibrates in its ion cage and occasionally hops out of the cage and diffuses.

To quantify the ion vibration inside the ion cage, the one-dimensional ion position distributions of cations and anions in their cages with respect to the center of mass of the cage were calculated, as plotted in Figure 4. It can be clearly seen that both cations and anions are trapped and vibrate in a small region of about ±2 Å. When a strong electric field is applied, the ion position distribution inside the cage is slightly biased along the X axis, but no bias is observed in the Y and Z axes. This again confirms the relaxation effect, with which the applied electric field is balanced by the dislocation of the central ion from the cage center.[68] In addition, as a result of ion cage

dx.doi.org/10.1021/jp311017r | J. Phys. Chem. B 2013, 117, 5102−5112

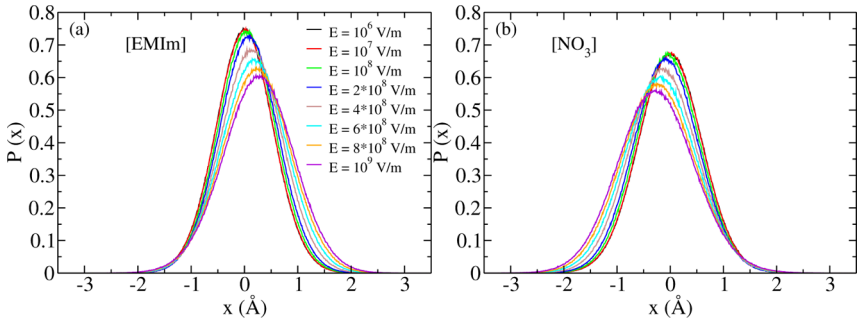

Figure 4. One-dimensional ion position distributions with respect to the center of mass of the ion cage in the field direction for cations (a) and anions (b) under various strengths of external electric fields.

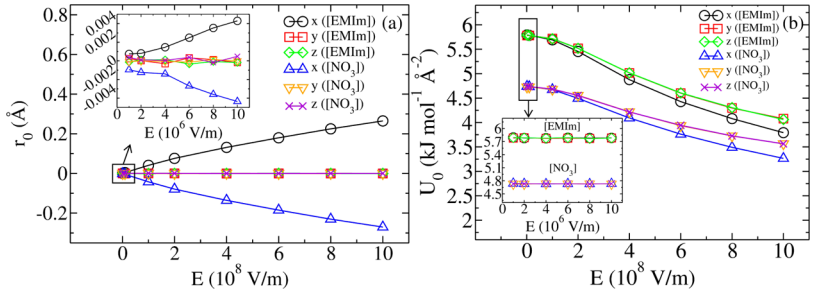

Figure 5. Effective cage potential shift r_0 (a) and strength U_0 (b) along different directions as a function of the electric field strength ranging from 10^6 to 10^9 V/m. Insets: enlarged plots for 10^6–10^7 V/m.

expansion, the ion position distributions become wider and the peak values are lower as the electric field increases. On the other hand, when a moderate electric field is applied, no noticeable changes of ion position distributions were observed.

The thermal vibration of an ion inside its cage can be considered as the confined movement of the ion in an effective cage potential well. Further examination shows that all the ion position distributions have a perfect Gaussian form (see section E in the Supporting Information). By fitting the ion position distributions with the Boltzmann distribution (eq 6), the effective potential experienced by the trapped ion can be described by the form

$$U(r) = U_0(r - r_0)^2 \tag{10}$$

where U_0 is the effective cage potential strength and r_0 is the position shift from the cage center. The shift r_0 as a function of electric field strength is plotted in Figure 5a. With a strong electric field applied, the ion cage with a central cation (anion) has a positive (negative) position shift along the X axis, suggesting that the electric fields tilt the effective cage potential well. As a result, the hopping rate for an ion to escape its cage becomes asymmetric along the electric field, leading to a unidirectional drift motion. In fact, the field-induced drift motion is observed in our simulations and we will discuss it later in section 4.2. Besides, the effective cage potential strength U_0 was found to decrease with the electric field strength in all three directions, as shown in Figure 5b. Due to the competition of the external electric field to the intrinsic electrostatic interactions, the ions tend to be more apart from each other. Since larger separation of ions reduces the ion−ion interaction,[58] the expansion of the ion cage weakens the effective cage potential. This explains why the effective cage potential strength and ion cage structure begin to change at the same strength of electric field. Moreover, the cation experiences a higher effective cage potential than the anion, possibly due to its larger size.

The cage potential shift and strength under moderate electric fields are plotted in the insets of Figure 5. It can be seen that the ion position distribution still shifts a very small distance in the order of 10^{-3} Å for both cation and anion, which indicates the tilt of cage potential well under moderate fields. In contrast, the cage potential strength shows no detectable changes, because a moderate electric field cannot change the ion cage structure in an influential way, as demonstrated in section 3.1.

Besides the tilt and weakening of the effective cage potential, under a strong electric field, the effective cage potential well becomes anisotropic for both cation and anion. It can be seen from Figure 5b that the cage potential strength U_0 becomes slightly lower along the field direction than the other two directions, whereas no differences were found between the Y and Z directions. This anisotropic cage potential can be attributed to the anisotropic deformation of the ion cage by the external field, which is also illustrated by the angle-resolved RDFs plotted in Figure S4 in the Supporting Information.

The effect of an external electric field on the ion cage structure is summarized as follows: (1) the ion position distribution in the cage is always biased, indicating a tilt of effective cage potential well; (2) a moderate electric field is too weak to change the ion cage structure and the effective cage potential in an influential way; (3) under a strong electric field, the ion cage expands and deforms, as schematically illustrated in Figure 6, thus leading to a weaker and anisotropic effective cage potential well.

Up to this point, we have shown how the external electric field changes the ion cage structure. In the following sections, we will demonstrate how these structural changes of the ion cage influence the dynamic properties of ILs and how the structural changes are associated with the dynamic changes.

dx.doi.org/10.1021/jp311017r | J. Phys. Chem. B 2013, 117, 5102−5112

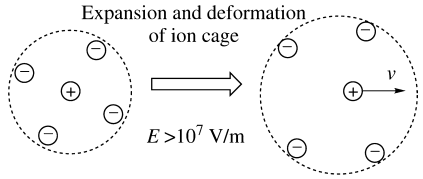

Figure 6. Schematic illustration of an ion cage in the absence (left) and presence (right) of a strong external electric field.

4. DYNAMIC CHANGES

4.1. Ion Cage Dynamics. A rational explanation of the relatively high viscosity of ILs is that ions are trapped in their cages for a long time before they occasionally hop out. To quantify this dynamic process, the TCF $C_{cage}(t)$ describing the relaxation of ion cage structure was calculated by eq 7. By definition, $C_{cage}(t)$ characterizes the probability of a cation and an anion that remain continuously in the same cage until time t, given that they stay in the same cage at time zero. Since $C_{cage}(t)$ is averaged over all ions in the cage, it actually describes the dynamics of the ion cage rather than an ion pair.[46,69] It can be seen from Figure 7 that $C_{cage}(t)$ decays much faster for a stronger electric field, which indicates that by pulling the cations and anions toward the opposite directions, the external electric field significantly accelerates the ion-escaping processes. On the other hand, as suggested by the overlap of $C_{cage}(t)$ at E = 10^6 and 10^7 V/m, a moderate electric field does not measurably change the ion cage dynamics.

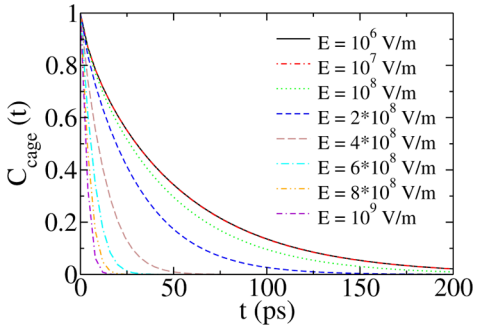

Figure 7. Time correlation functions of ion cage dynamics with various strengths of external electric fields. The curve for E = 10^6 V/m overlaps exactly with the curve for E = 10^7 V/m.

The ion cage structure plays an important role in determining the dynamics of ions, and in turn, the ion cage dynamics can also influence the ion cage structure, because the central ion and its cage are strongly correlated: the ion that is caged by its neighbors also behaves as a cage member of its neighbors. Therefore, the ion cage relaxation should be regarded as a correlated rather than individual behavior of ions.[48] From this perspective, the expansion and deformation of ion cage discussed in the previous sections can be understood as follows. Without an external field, the ion is usually long-time trapped in its cage due to the very strong electric attraction between the central ion and its cage; under a strong electric field, when the central ion frequently escapes the cage, the counterions repulse each other and the ion cage expands. Besides, the counterions are pushed away from a central ion perpendicular to the field direction to allow the central ion to drift along the field direction, which results in an anisotropic deformation of the ion cage.

On the basis of the above discussion, we propose that the central ion and its ion cage are highly correlated in ILs: owing to the fast ion cage dynamics at strong external electric fields, the ion cage expands and deforms through collective rearrangement of ions, which further influences the dynamic properties of ILs. In the following sections, we will discuss the effect of electric field on the ion mobility and self-diffusion of [EMIm][NO_3] in detail.

4.2. Ion Mobility. The ion drift velocity and the related mobility are essential quantities for characterizing the transport property of ILs. However, since the feeble drift motion is usually submerged in the vibrant thermal motion, it is very difficult to measure in experiment and to calculate in simulation. With the method described in section 2.2, we managed to determine in MD simulation the drift velocity at both moderate and strong electric fields, as shown in Figure 8.

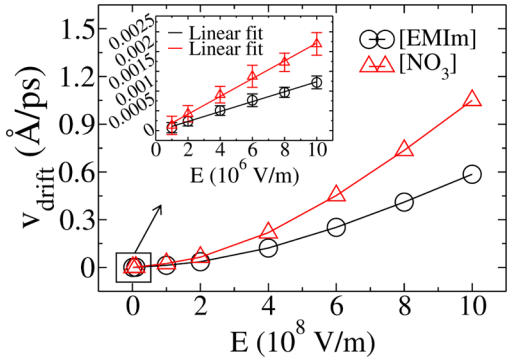

Figure 8. Drift velocities as a function of electric field strength ranging from 10^6 to 10^9 V/m. Inset: enlarged plot for 10^6–10^7 V/m. The error bars show the standard deviations of drift velocities, which are too small to be seen at strong electric fields.

The drift velocity grows almost linearly in the range of moderate electric fields but increases rapidly and nonlinearly at strong electric fields. This indicates that the system remains in a linear-response region (near equilibrium) until a strong electric field is applied.

The ion mobility, describing the moving ability of ions in response to the external electric field, was calculated from the drift velocity according to eq 8. As shown in Figure 9, the ion mobility keeps constant at moderate fields, since the effective

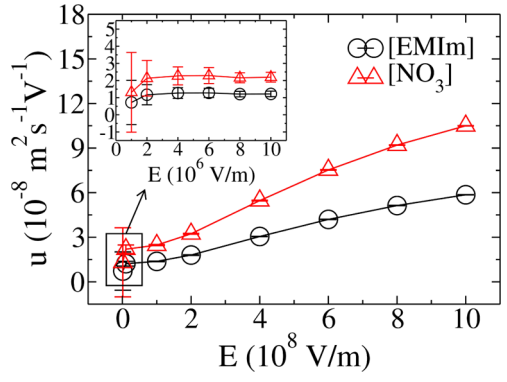

Figure 9. Ion mobilities of cations and anions as a function of electric field strength ranging from 10^6 to 10^9 V/m. Inset: enlarged plot for 10^6–10^7 V/m. The error bars show the standard deviations of ion mobilities, which are too small to be seen at strong electric fields.

dx.doi.org/10.1021/jp311017r | J. Phys. Chem. B 2013, 117, 5102–5112

cage potential well and the underlying ion cage structure have no detectable changes under moderate electric fields. On the other hand, at strong electric fields, the expansion of the ion cage effectively promotes the drift motion by weakening the effective cage potential and thus allows the trapped ions to escape the cage much easier. As a result, the ion mobilities of cations and anions both increase gradually but apparently with electric field. Both smaller volume and lighter mass of anion favor a faster drift motion of anion than cation.

4.3. Self-Diffusion. By deducting the drift motion from the mean-square displacement of ions (see section H in the Supporting Information), the effective self-diffusion coefficients were calculated with eq 9, as plotted in Figure 10. Similar to the

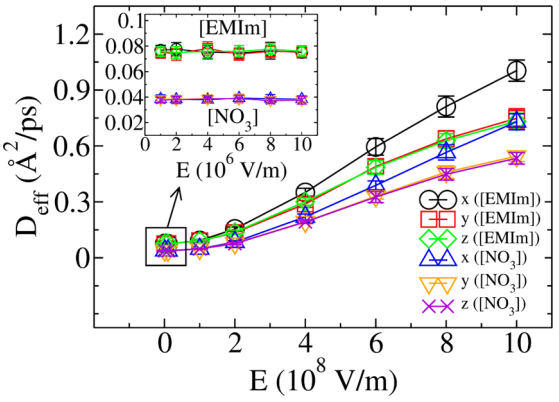

Figure 10. One-dimensional effective self-diffusion coefficients as a function of electric field strength ranging from 10^6 to 10^9 V/m. Inset: enlarged plot for 10^6–10^7 V/m. The error bars represent the standard deviations.

change of mobility, the self-diffusion gradually and significantly increases at strong electric fields but remains a constant at moderate electric fields. Along with the previous discussion on the ion cage structure, the effect of external electric field on the dynamic properties of ILs can be consistently understood by the changes of ion cage structure: under a moderate electric field, the mobility and self-diffusion coefficient remain constant, since the moderate electric field is too weak to change the ion cage structure in an influential way; under a strong electric field, the electric field induces the expansion of the ion cage, and thus weakens the effective cage potential, leading to the increase of both mobility and self-diffusion of ions. At strong electric fields, as a result of the anisotropic deformation of the ion cage, the diffusion along the field direction is faster than the other two directions.

Another proposed mechanism[12] postulates that the external electric field aligns the ions to provide ion transport pathways accelerating the dynamics along the field direction. Our results, however, strongly discourage that mechanism based on two facts: (1) as we show in section G in the Supporting Information, the field-induced orientational ordering of cations is not very large even at very strong fields; (2) the ion alignment mechanism would lead to a slower dynamics in the direction perpendicular to the electric field, but our analysis has shown that the effective self-diffusion increases with electric field in all three directions. Therefore, it is the ion cage structure rather than the orientational ordering that determines the changes of the dynamic properties of ILs.

5. DISCUSSION

5.1. Microscopic Mechanism. The structural and dynamic changes of [EMIm][NO_3] under an external electric field can be systematically explained by a microscopic mechanism based on the statistical concept of *ion cage*. In this mechanism, an ion vibrates inside an effective cage potential well and occasionally jumps out of the potential well by climbing over its energy barrier. The minimum energy that an ion needs to climb over the energy barrier (height of the effective cage potential well) is called the activation energy, which determines the dynamic properties of the system: lower activation energy allows an ion to escape easier and hence the ion diffuses faster. We estimated the activation energy in the system by fitting the self-diffusion coefficients to the Arrhenius law. As shown in section I in the Supporting Information, the activation energy decreases apparently at strong electric fields but remains constant at weak and moderate electric fields. Moreover, the activation energy in the field direction becomes lower than the other two directions at strong electric fields. The changes of the effective cage potential well under an external electric field are schematically illustrated in Figure 11.

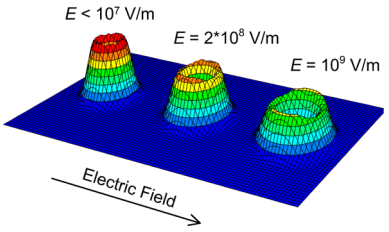

Figure 11. Schematic illustration of the effective cage potential well at different strengths of external electric fields.

When a weak or moderate electric field is applied, the underlying ion cage structure and hence the dynamic properties show no measurable changes, since the external electric field is too weak to compete with the intrinsic electric field in ILs as strong as 10^9 V/m.[58] Under a strong external electric field, the ion cage expands due to the competition of the external electric field to the intrinsic electrostatic interactions, which effectively lowers the energy barrier of the cage potential well and thus accelerates the ion mobility and self-diffusion. The strong external electric field also deforms the ion cage to be anisotropic, so the effective cage potential well and hence the self-diffusion become anisotropic with lower energy barrier and faster diffusion in the field direction than the other two directions.

Meanwhile, the effective ion cage potential well is always tilted under an external electric field regardless of its strength, as evidenced by the bias of the ion position distribution in the ion cage. Although quite weak, we managed to observe the bias in the order of 10^{-3} Å under a moderate electric field (see Figures 4 and 5a). In the absence of an external electric field, the ions have equal probabilities to hop out of the effective cage potential well in any direction. When an electric field is applied, the effective cage potential well is tilted and hence the symmetry of the hopping motion along the field direction is broken. Cations have a slightly higher probability to hop out forward in the electric field direction, while anions tend to hop backward, which leads to a net ionic current in the system. Although the tilt is usually too small to be observed under a weak external electric field, thanks to the feeble but persistent

dx.doi.org/10.1021/jp311017r | J. Phys. Chem. B 2013, 117, 5102–5112

tilt of the effective cage potential well, the microscopic asymmetric ion hops are accumulated to generate the macroscopic ionic current.

5.2. Breakdown of the Einstein Relation. The Einstein relation is an important theorem which connects mobility with self-diffusion by assuming that liquid particles have weak correlations. For a multicomponent system, if particles move independently and the system stays in a linear-response region, the Einstein relation holds for each species.[70−72] For simplicity, we define the scaled mobility for each species i as

$$u_i' = u_i k_B T/ze \tag{11}$$

and thus the Einstein relation (eq 1) is simplified as

$$D_i = u_i' \tag{12}$$

Nevertheless, due to strong ion−ion coupling, the applicability of the Einstein relation to ILs is questionable. Although the validities of the derived Stokes−Einstein and Nernst−Einstein relations have been widely studied,[73−81] the validity of the more fundamental Einstein relation for ILs still remains elusive due to the difficulty of determining ion mobility in ILs under a weak or moderate electric field. Since in this work we have managed to calculate ion mobility at moderate and strong electric fields, we can check directly the validity of the Einstein relation for a single ion species (eq 12) as well as for the whole system (all ions) ($D_+ + D_- = u_+' + u_-'$) in [EMIm][NO_3].

Unlike several studies[74−77] indicating that the correlated ion motions in ILs deviate from the Nernst−Einstein relation, the overall scaled mobility ($u_+' + u_-'$) and the overall self-diffusion coefficient ($D_+ + D_-$) for all ions approximately obey the Einstein relation under a moderate electric field (linear-response region), as shown in section J in the Supporting Information. However, due to the large statistical errors in our simulation data, we cannot be certain if the Einstein relation still holds for all ions in the linear-response region. On the other hand, for a single ion species (cation or anion), we found that the Einstein relation clearly breaks down at both moderate and strong electric fields, as shown in Figure 12. (In the moderate field region, we only show the data for $E = 10^7$ V/m, because both mobility and self-diffusion keep constant in this region.) Besides the expected breakdown at strong electric fields, surprisingly, the Einstein relation also breaks down for each ion species even in the linear-response region, which may be attributed to the strong correlation of ion motions in the IL system.

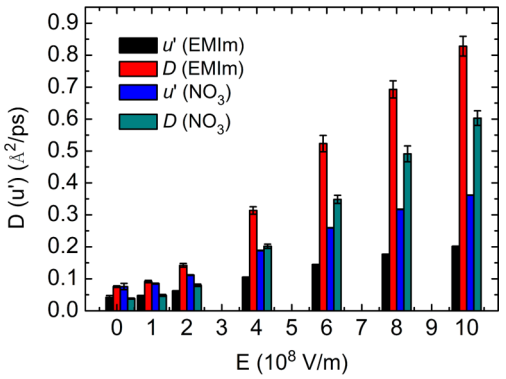

Figure 12. Comparison of self-diffusion and mobility indicating the breakdown of the Einstein relation. The bars around $E = 0$ V/m represent the data for $E = 10^7$ V/m.

At strong fields (far from equilibrium), the Einstein relation apparently breaks down for the whole system as well as for each ion species. Moreover, the relation between diffusion and mobility is different for cation and anion. For cation, the diffusion coefficient is always larger than mobility, possibly because its chain-like structure helps the thermal-driven diffusion but its large size retards the field-driven drift motion. For anion, in contrast, at a moderate electric field, mobility becomes larger than the diffusion coefficient because its small volume allows it to stay in the ion cage for a long time but, along with its light mass, also allows it to be easily driven by the electric field. This tendency for anion turns over when the electric field is larger than 2×10^8 V/m, because the diffusion coefficient increases faster than mobility with increasing external field, as illustrated in Figures 9 and 10.

5.3. Structure and Dynamics under a Weak Electric Field. In the previous sections, we have discussed in detail the simulated structure and dynamics of [EMIm][NO_3] under moderate and strong electric fields and have proposed a mechanism based on the ion cage structure to explain those observations. Since most experiments were performed at weak electric fields, it is necessary for us to investigate the structural and dynamic properties of [EMIm][NO_3] under weak electric fields.

As stated above, the ion cage plays an essential role in determining the structure and dynamics of ILs under an external electric field. Since the ion cage does not have detectable alteration even at a moderate electric field, we may assert that the ion cage structure and related dynamic properties remain unchanged at weak electric fields. This assertion is supported by our calculated RDF, ion position distribution, bulk density, effective cage potential strength, cationic orientation, ion cage dynamics, and self-diffusion coefficient of [EMIm][NO_3]. As shown in section K in the Supporting Information, all of the above properties exhibit no observable changes within the statistical errors, when the applied electric field increases from 0 to 10^6 V/m. This assertion is also supported by our calculated conductivities, which remain almost constant in the absence and presence of moderate electric fields (see section L in the Supporting Information for details). This is not surprising if we compare the external electric field with the very strong intrinsic electric fields in ILs, which has been determined to be in the order of 10^9 V/m.[58]

In contrast to our conclusions, some experimental groups claimed that they observed the increase of mobility and self-diffusion coefficient in several ILs at very weak electric fields (0−400 V/m). In particular, by using the low-voltage electrophoretic NMR technique, Hayamizu et al.[11] observed a gradual increase of self-diffusion coefficients in ILs with electric field strength (0−300 V/m). Moreover, the self-diffusion coefficient was found to be time dependent: it first increases to a peak value and then decays slowly with time. This implies that the system may not be in a steady state during the NMR measurement. When an electric field is applied, cations and anions move to the negative and positive electrodes, respectively, forming the electric double layer on the electrodes. Thus, the output signal reflects the local concentration gradients near the electrodes rather than the self-diffusion of the bulk IL in a nonequilibrium steady state.

dx.doi.org/10.1021/jp311017r | J. Phys. Chem. B 2013, 117, 5102−5112

In another NMR experiment, by assuming that the self-diffusion coefficient is independent of the applied electric field, Saito et al.[12] found a sudden increase of ion mobility by 1 order of magnitude in several ILs and proposed a mechanism of the transport pathway formed by the ion alignment along the electric field to explain their experimental results. However, their assumption actually conflicts with Hayamizu's NMR experiment results showing that the self-diffusion coefficient gradually increases with electric field, and as described in section 4.3, our simulation results have also ruled out the orientation ordering in ILs under a weak electric field. In fact, their assumption of the independence of the self-diffusion coefficient with the applied electric field is quite questionable, leading to their conclusions being contradictory with another experiment and our suggested mechanism.

Note that in a real setup the electric field is usually applied between two electrodes. Therefore, besides the ion cage, the interfacial structure of ILs at the electrodes may also play a role in determining the nonequilibrium behavior of ILs. Combining the ion-cage structure in the bulk and the layer structure at the electrode interfaces could be the subject of future investigations.

6. CONCLUSIONS

In the present paper, the nonequilibrium steady state of the [EMIm][NO_3] IL driven by an external electric field (0−10^9 V/m) was investigated by nonequilibrium CG MD simulations. In order to understand the microscopic mechanism for the structural and dynamic changes of ILs when an electric field is applied, a number of structural properties and their field dependence were studied and interpreted by an "ion cage" mechanism: under weak and moderate electric fields ($0 < E \leq 10^7$ V/m), the ion cage structure remains unchanged, since the external electric field is too weak to compete with the intrinsic electric field in ILs as strong as 10^9 V/m; under a strong electric field (10^7 V/m $< E \leq 10^9$ V/m), the ion cage expands and deforms anisotropically, resulting in a lower and anisotropic cage potential well.

An effective approach was successfully introduced to calculate the drift velocity under moderate and strong electric fields by eliminating the dominating random self-diffusion velocities. The ion cage dynamics, mobility, and effective self-diffusion coefficient were calculated and analyzed in detail. The changes of the dynamic properties of ILs under an external electric field are interpreted by the changes of the ion cage structure: under weak and moderate electric fields, the dynamic properties stay unchanged, since the applied electric field is too weak to alter the ion cage structure; under a strong electric field, the electric field induces the expansion of the ion cage, which effectively lowers the energy barrier of the cage potential well and thus leads to the enhancement of mobility and self-diffusion of ions. The anisotropic deformation of the ion cage structure results in faster diffusion in the direction along the electric field. In addition, the Einstein relation connecting diffusion and mobility breaks down at strong electric fields, and we found that it also breaks down for a single ion species even at moderate electric fields (linear-response region).

By employing the statistical concept of ion cage, this work suggested a detailed microscopic mechanism to systematically explain the structural and dynamic changes of ILs under an external electric field, as well as to help better understand experimental results. The suggested mechanism is anticipated to further advance our knowledge of the effect of an external electric field on the behavior of ILs and help the applications of ILs in nonequilibrium conditions, such as electrochemical devices.

■ ASSOCIATED CONTENT

Supporting Information

Various results supporting the data analysis in the main text. This material is available free of charge via the Internet at http://pubs.acs.org.

■ AUTHOR INFORMATION

Corresponding Author

*Phone: +86 10-62648749. E-mail: wangyt@itp.ac.cn.

Notes

The authors declare no competing financial interest.

■ ACKNOWLEDGMENTS

This work was supported by the National Natural Science Foundation of China (No. 10974208 and No. 11121403) and the Hundred Talent Program of the Chinese Academy of Sciences (CAS). The authors thank the Supercomputing Center in the Computer Network Information Center at the CAS for allocations of computer time.

■ REFERENCES

(1) Welton, T. Room-Temperature Ionic Liquids. Solvents for Synthesis and Catalysis. *Chem. Rev.* **1999**, *99*, 2071−2084.
(2) Wasserscheid, P.; Welton, T. *Ionic Liquids in Synthesis*; Wiley-VCH: Weinheim, Germany, 2008.
(3) Rogers, R. D.; Seddon, K. R. Ionic Liquids - Solvents of the Future? *Science* **2003**, *302*, 792−793.
(4) Plechkova, N. V.; Seddon, K. R. Applications of Ionic Liquids in the Chemical Industry. *Chem. Soc. Rev.* **2008**, *37*, 123−150.
(5) Armand, M.; Endres, F.; MacFarlane, D. R.; Ohno, H.; Scrosati, B. Ionic-Liquid Materials for the Electrochemical Challenges of the Future. *Nat. Mater.* **2009**, *8*, 621−629.
(6) Seki, S.; Kobayashi, Y.; Miyashiro, H.; Ohno, Y.; Usami, A.; Mita, Y.; Kihira, N.; Watanabe, M.; Terada, N. Lithium Secondary Batteries Using Modified-Imidazolium Room-Temperature Ionic Liquid. *J. Phys. Chem. B* **2006**, *110*, 10228−10230.
(7) de Souza, R. F.; Padilha, J. C.; Gonçalves, R. S.; Dupont, J. Room Temperature Dialkylimidazolium Ionic Liquid-Based Fuel Cells. *Electrochem. Commun.* **2003**, *5*, 728−731.
(8) Gamero-Castano, M.; Hruby, V. Electrospray as a Source of Nanoparticles for Efficient Colloid Thrusters. *J. Propul. Power* **2001**, *17*, 977−987.
(9) Yanes, E. G.; Gratz, S. R.; Baldwin, M. J.; Robison, S. E.; Stalcup, A. M. Capillary Electrophoretic Application of 1-Alkyl-3-Methylimidazolium-Based Ionic Liquids. *Anal. Chem.* **2001**, *73*, 3838−3844.
(10) Hapiot, P.; Lagrost, C. Electrochemical Reactivity in Room-Temperature Ionic Liquids. *Chem. Rev.* **2008**, *108*, 2238−2264.
(11) Hayamizu, K.; Aihara, Y. Correlating the Ionic Drift under Pt/Pt Electrodes for Ionic Liquids Measured by Low-Voltage Electrophoretic NMR with Chronoamperometry. *J. Phys. Chem. Lett.* **2010**, *1*, 2055−2058.
(12) Umecky, T.; Saito, Y.; Matsumoto, H. Direct Measurements of Ionic Mobility of Ionic Liquids Using the Electric Field Applying Pulsed Gradient Spin−Echo NMR. *J. Phys. Chem. B* **2009**, *113*, 8466−8468.
(13) Borner, A.; Li, Z.; Levin, D. A. Modeling of an Ionic Liquid Electrospray Using Molecular Dynamics with Constraints. *J. Chem. Phys.* **2012**, *136*, 124507.
(14) Daily, J. W.; Micci, M. M. Ionic Velocities in an Ionic Liquid under High Electric Fields Using All-Atom and Coarse-Grained Force Field Molecular Dynamics. *J. Chem. Phys.* **2009**, *131*, 094501.

(15) English, N. J.; Mooney, D. A. Very Different Responses to Electromagnetic Fields in Binary Ionic Liquid-Water Solutions. *J. Phys. Chem. B* **2009**, *113*, 10128−10134.
(16) English, N. J.; Mooney, D. A.; O'Brien, S. Ionic Liquids in External Electric and Electromagnetic Fields: A Molecular Dynamics Study. *Mol. Phys.* **2011**, *109*, 625−638.
(17) Petravic, J.; Delhommelle, J. Conductivity of Molten Sodium Chloride and Its Supercritical Vapor in Strong dc Electric Fields. *J. Chem. Phys.* **2003**, *118*, 7477−7485.
(18) Sha, M.; Niu, D.; Dou, Q.; Wu, G.; Fang, H.; Hu, J. Reversible Tuning of the Hydrophobic-Hydrophilic Transition of Hydrophobic Ionic Liquids by Means of an Electric Field. *Soft Matter* **2011**, *7*, 4228−4233.
(19) Wang, Y. Disordering and Reordering of Ionic Liquids under an External Electric Field. *J. Phys. Chem. B* **2009**, *113*, 11058−11060.
(20) Zhao, H.; Shi, R.; Wang, Y. Nanoscale Tail Aggregation in Ionic Liquids: Roles of Electrostatic and Van Der Waals Interactions. *Commun. Theor. Phys.* **2011**, *56*, 499−503.
(21) Hayes, R.; Borisenko, N.; Tam, M. K.; Howlett, P. C.; Endres, F.; Atkin, R. Double Layer Structure of Ionic Liquids at the Au(111) Electrode Interface: An Atomic Force Microscopy Investigation. *J. Phys. Chem. C* **2011**, *115*, 6855−6863.
(22) Mezger, M.; Schröder, H.; Reichert, H.; Schramm, S.; Okasinski, J. S.; Schöder, S.; Honkimäki, V.; Deutsch, M.; Ocko, B. M.; Ralston, J.; et al. Molecular Layering of Fluorinated Ionic Liquids at a Charged Sapphire (0001) Surface. *Science* **2008**, *322*, 424−428.
(23) Sha, M.; Wu, G.; Dou, Q.; Tang, Z.; Fang, H. Double-Layer Formation of [Bmim][Pf6] Ionic Liquid Triggered by Surface Negative Charge. *Langmuir* **2010**, *26*, 12667−12672.
(24) Fedorov, M. V.; Kornyshev, A. A. Towards Understanding the Structure and Capacitance of Electrical Double Layer in Ionic Liquids. *Electrochim. Acta* **2008**, *53*, 6835−6840.
(25) Fedorov, M. V.; Georgi, N.; Kornyshev, A. A. Double Layer in Ionic Liquids: The Nature of the Camel Shape of Capacitance. *Electrochem. Commun.* **2010**, *12*, 296−299.
(26) Georgi, N.; Kornyshev, A. A.; Fedorov, M. V. The Anatomy of the Double Layer and Capacitance in Ionic Liquids with Anisotropic Ions: Electrostriction Vs. Lattice Saturation. *J. Electroanal. Chem.* **2010**, *649*, 261−267.
(27) Fedorov, M. V.; Kornyshev, A. A. Ionic Liquid near a Charged Wall: Structure and Capacitance of Electrical Double Layer. *J. Phys. Chem. B* **2008**, *112*, 11868−11872.
(28) Feng, G.; Zhang, J. S.; Qiao, R. Microstructure and Capacitance of the Electrical Double Layers at the Interface of Ionic Liquids and Planar Electrodes. *J. Phys. Chem. C* **2009**, *113*, 4549−4559.
(29) Lynden-Bell, R. M.; Frolov, A. I.; Fedorov, M. V. Electrode Screening by Ionic Liquids. *Phys. Chem. Chem. Phys.* **2012**, *14*, 2693−2701.
(30) Shim, Y.; Kim, H. J.; Jung, Y. Graphene-Based Supercapacitors in the Parallel-Plate Electrode Configuration: Ionic Liquids Versus Organic Electrolytes. *Faraday Discuss.* **2012**, *154*, 249−263.
(31) Shim, Y.; Jung, Y.; Kim, H. J. Graphene-Based Supercapacitors: A Computer Simulation Study. *J. Phys. Chem. C* **2011**, *115*, 23574−23583.
(32) Vatamanu, J.; Borodin, O.; Smith, G. D. Molecular Insights into the Potential and Temperature Dependences of the Differential Capacitance of a Room-Temperature Ionic Liquid at Graphite Electrodes. *J. Am. Chem. Soc.* **2010**, *132*, 14825−14833.
(33) Vatamanu, J.; Borodin, O.; Smith, G. D. Molecular Simulations of the Electric Double Layer Structure, Differential Capacitance, and Charging Kinetics for N-Methyl-N-Propylpyrrolidinium Bis-(fluorosulfonyl)imide at Graphite Electrodes. *J. Phys. Chem. B* **2011**, *115*, 3073−3084.
(34) Si, X.; Li, S.; Wang, Y.; Ye, S.; Yan, T. Effects of Specific Adsorption on the Differential Capacitance of Imidazolium-Based Ionic Liquid Electrolytes. *ChemPhysChem* **2012**, *13*, 1671−1676.
(35) Pinilla, C.; Del Pópolo, M. G.; Kohanoff, J.; Lynden-Bell, R. M. Polarization Relaxation in an Ionic Liquid Confined between Electrified Walls. *J. Phys. Chem. B* **2007**, *111*, 4877−4884.
(36) Merlet, C.; Rotenberg, B.; Madden, P. A.; Taberna, P.-L.; Simon, P.; Gogotsi, Y.; Salanne, M. On the Molecular Origin of Supercapacitance in Nanoporous Carbon Electrodes. *Nat. Mater.* **2012**, *11*, 306−310.
(37) Merlet, C.; Péan, C.; Rotenberg, B.; Madden, P. A.; Simon, P.; Salanne, M. Simulating Supercapacitors: Can We Model Electrodes as Constant Charge Surfaces? *J. Phys. Chem. Lett.* **2013**, *4*, 264−268.
(38) Xing, L.; Vatamanu, J.; Borodin, O.; Bedrov, D. On the Atomistic Nature of Capacitance Enhancement Generated by Ionic Liquid Electrolyte Confined in Subnanometer Pores. *J. Phys. Chem. Lett.* **2013**, *4*, 132−140.
(39) Polissar, M. J. A Kinetic Approach to the Theory of Conductance of Infinitely Dilute Solutions, Based on the "Cage" Model of Liquids. *J. Chem. Phys.* **1938**, *6*, 833−844.
(40) Gezelter, J. D.; Rabani, E.; Berne, B. J. Calculating the Hopping Rate for Diffusion in Molecular Liquids: CS_2. *J. Chem. Phys.* **1999**, *110*, 3444−3452.
(41) Rabani, E.; Gezelter, J. D.; Berne, B. J. Calculating the Hopping Rate for Self-Diffusion on Rough Potential Energy Surfaces: Cage Correlations. *J. Chem. Phys.* **1997**, *107*, 6867−6876.
(42) Cavagna, A. Supercooled Liquids for Pedestrians. *Phys. Rep.* **2009**, *476*, 51−124.
(43) Turton, D. A.; Hunger, J.; Stoppa, A.; Thoman, A.; Candelaresi, M.; Hefter, G.; Walther, M.; Buchner, R.; Wynne, K. Rattling the Cage: Micro- to Mesoscopic Structure in Liquids as Simple as Argon and as Complicated as Water. *J. Mol. Liq.* **2011**, *159*, 2−8.
(44) Margulis, C. J.; Stern, H. A.; Berne, B. J. Computer Simulation of a "Green Chemistry" Room-Temperature Ionic Solvent. *J. Phys. Chem. B* **2002**, *106*, 12017−12021.
(45) Morrow, T. I.; Maginn, E. J. Molecular Dynamics Study of the Ionic Liquid 1-n-Butyl-3-methylimidazolium Hexafluorophosphate. *J. Phys. Chem. B* **2002**, *106*, 12807−12813.
(46) Kohagen, M.; Brehm, M.; Thar, J.; Zhao, W.; Müller-Plathe, F.; Kirchner, B. Performance of Quantum Chemically Derived Charges and Persistence of Ion Cages in Ionic Liquids. A Molecular Dynamics Simulations Study of 1-n-Butyl-3-methylimidazolium Bromide. *J. Phys. Chem. B* **2010**, *115*, 693−702.
(47) Del Pópolo, M. G.; Voth, G. A. On the Structure and Dynamics of Ionic Liquids. *J. Phys. Chem. B* **2004**, *108*, 1744−1752.
(48) Schröder, C. Collective Translational Motions and Cage Relaxations in Molecular Ionic Liquids. *J. Chem. Phys.* **2011**, *135*, 024502.
(49) Habasaki, J.; Ngai, K. L. Heterogeneous Dynamics of Ionic Liquids from Molecular Dynamics Simulations. *J. Chem. Phys.* **2008**, *129*, 194501.
(50) Hu, Z.; Margulis, C. J. Heterogeneity in a Room-Temperature Ionic Liquid: Persistent Local Environments and the Red-Edge Effect. *Proc. Natl. Acad. Sci. U.S.A.* **2006**, *103*, 831−836.
(51) Singh, R.; Monk, J.; Hung, F. R. Heterogeneity in the Dynamics of the Ionic Liquid $[BMIM^+][PF_6^-]$ Confined in a Slit Nanopore. *J. Phys. Chem. C* **2011**, *115*, 16544−16554.
(52) Karimi-Varzaneh, H. A.; Müller-Plathe, F.; Balasubramanian, S.; Carbone, P. Studying Long-Time Dynamics of Imidazolium-Based Ionic Liquids with a Systematically Coarse-Grained Model. *Phys. Chem. Chem. Phys.* **2010**, *12*, 4714−4724.
(53) Turton, D. A.; Hunger, J.; Stoppa, A.; Hefter, G.; Thoman, A.; Walther, M.; Buchner, R.; Wynne, K. Dynamics of Imidazolium Ionic Liquids from a Combined Dielectric Relaxation and Optical Kerr Effect Study: Evidence for Mesoscopic Aggregation. *J. Am. Chem. Soc.* **2009**, *131*, 11140−11146.
(54) Hardacre, C.; Holbrey, J. D.; McMath, S. E. J.; Bowron, D. T.; Soper, A. K. Structure of Molten 1,3-Dimethylimidazolium Chloride Using Neutron Diffraction. *J. Chem. Phys.* **2003**, *118*, 273−278.
(55) Deetlefs, M.; Hardacre, C.; Nieuwenhuyzen, M.; Padua, A. A. H.; Sheppard, O.; Soper, A. K. Liquid Structure of the Ionic Liquid 1,3-Dimethylimidazolium Bis{(trifluoromethyl)sulfonyl}amide. *J. Phys. Chem. B* **2006**, *110*, 12055−12061.

(56) Bhargava, B. L.; Klein, M. L.; Balasubramanian, S. Structural Correlations and Charge Ordering in a Room-Temperature Ionic Liquid. *ChemPhysChem* **2008**, *9*, 67−70.
(57) Siqueira, L. J. A.; Ribeiro, M. C. C. Charge Ordering and Intermediate Range Order in Ammonium Ionic Liquids. *J. Chem. Phys.* **2011**, *135*, 204506.
(58) Zhang, S.; Shi, R.; Ma, X.; Lu, L.; He, Y.; Zhang, X.; Wang, Y.; Deng, Y. Intrinsic Electric Fields in Ionic Liquids Determined by Vibrational Stark Effect Spectroscopy and Molecular Dynamics Simulation. *Chem.—Eur. J.* **2012**, *18*, 11904−11908.
(59) Wang, Y.; Feng, S.; Voth, G. A. Transferable Coarse-Grained Models for Ionic Liquids. *J. Chem. Theory Comput.* **2009**, *5*, 1091−1098.
(60) Wang, Y.; Noid, W. G.; Liu, P.; Voth, G. A. Effective Force Coarse-Graining. *Phys. Chem. Chem. Phys.* **2009**, *11*, 2002−2015.
(61) Forester, T. R.; Smith, W. *Dl_Poly User Manual*; CCLRC, Daresbury Laboratory: Daresbury, Warrington, U.K., 1995.
(62) Hoover, W. G. Canonical Dynamics: Equilibrium Phase-Space Distributions. *Phys. Rev. A* **1985**, *31*, 1695−1697.
(63) Nose, S. A Unified Formulation of the Constant Temperature Molecular Dynamics Methods. *J. Chem. Phys.* **1984**, *81*, 511−519.
(64) Blickle, V.; Speck, T.; Lutz, C.; Seifert, U.; Bechinger, C. Einstein Relation Generalized to Nonequilibrium. *Phys. Rev. Lett.* **2007**, *98*, 210601.
(65) Lindenberg, K.; Lacasta, A. M.; Sancho, J. M.; Romero, A. H. Transport and Diffusion on Crystalline Surfaces under External Forces. *New J. Phys.* **2005**, *7*, 29.
(66) Reimann, P.; Van den Broeck, C.; Linke, H.; Hänggi, P.; Rubi, J. M.; Pérez-Madrid, A. Giant Acceleration of Free Diffusion by Use of Tilted Periodic Potentials. *Phys. Rev. Lett.* **2001**, *87*, 010602.
(67) Zhao, W.; Leroy, F.; Heggen, B.; Zahn, S.; Kirchner, B.; Balasubramanian, S.; Müller-Plathe, F. Are There Stable Ion-Pairs in Room-Temperature Ionic Liquids? Molecular Dynamics Simulations of 1-n-Butyl-3-methylimidazolium Hexafluorophosphate. *J. Am. Chem. Soc.* **2009**, *131*, 15825−15833.
(68) Atkins, P.; de Paula, J. *Atkins' Physical Chemistry*, 7th ed.; Oxford University Press: Oxford, U.K., 2002.
(69) Kohagen, M.; Brehm, M.; Lingscheid, Y.; Giernoth, R.; Sangoro, J.; Kremer, F.; Naumov, S.; Iacob, C.; Kärger, J.; Valiullin, R.; et al. How Hydrogen Bonds Influence the Mobility of Imidazolium-Based Ionic Liquids. A Combined Theoretical and Experimental Study of 1-n-Butyl-3-methylimidazolium Bromide. *J. Phys. Chem. B* **2011**, *115*, 15280−15288.
(70) Borucka, A. Z.; Bockris, J. O. M.; Kitchener, J. A. Self-Diffusion in Molten Sodium Chloride: A Test of the Applicability of the Nernst-Einstein Equation. *Proc. R. Soc. London, Ser. A* **1957**, *241*, 554−567.
(71) Videa, M.; Xu, W.; Geil, B.; Marzke, R.; Angell, C. A. High Li^+ Self-Diffusivity and Transport Number in Novel Electrolyte Solutions. *J. Electrochem. Soc.* **2001**, *148*, A1352−A1356.
(72) Levine, I. N. *Physical Chemistry*, 6th ed.; McGraw-Hill: New York, 2009.
(73) Köddermann, T.; Ludwig, R.; Paschek, D. On the Validity of Stokes−Einstein and Stokes−Einstein−Debye Relations in Ionic Liquids and Ionic-Liquid Mixtures. *ChemPhysChem* **2008**, *9*, 1851−1858.
(74) Harris, K. R.; Kanakubo, M.; Tsuchihashi, N.; Ibuki, K.; Ueno, M. Effect of Pressure on the Transport Properties of Ionic Liquids: 1-Alkyl-3-methylimidazolium Salts. *J. Phys. Chem. B* **2008**, *112*, 9830−9840.
(75) Kanakubo, M.; Harris, K. R.; Tsuchihashi, N.; Ibuki, K.; Ueno, M. Effect of Pressure on Transport Properties of the Ionic Liquid 1-Butyl-3-methylimidazolium Hexafluorophosphate. *J. Phys. Chem. B* **2007**, *111*, 2062−2069.
(76) Kashyap, H. K.; Annapureddy, H. V. R.; Raineri, F. O.; Margulis, C. J. How Is Charge Transport Different in Ionic Liquids and Electrolyte Solutions? *J. Phys. Chem. B* **2011**, *115*, 13212−13221.
(77) Harris, K. R. Relations between the Fractional Stokes−Einstein and Nernst−Einstein Equations and Velocity Correlation Coefficients in Ionic Liquids and Molten Salts. *J. Phys. Chem. B* **2010**, *114*, 9572−9577.
(78) Jeong, D.; Choi, M. Y.; Kim, H. J.; Jung, Y. Fragility, Stokes-Einstein Violation, and Correlated Local Excitations in a Coarse-Grained Model of an Ionic Liquid. *Phys. Chem. Chem. Phys.* **2010**, *12*, 2001−2010.
(79) Noda, A.; Hayamizu, K.; Watanabe, M. Pulsed-Gradient Spin−Echo ^1H and ^{19}F NMR Ionic Diffusion Coefficient, Viscosity, and Ionic Conductivity of Non-Chloroaluminate Room-Temperature Ionic Liquids. *J. Phys. Chem. B* **2001**, *105*, 4603−4610.
(80) Tokuda, H.; Hayamizu, K.; Ishii, K.; Susan, M. A. B. H.; Watanabe, M. Physicochemical Properties and Structures of Room Temperature Ionic Liquids. 1. Variation of Anionic Species. *J. Phys. Chem. B* **2004**, *108*, 16593−16600.
(81) Liu, H.; Maginn, E. A Molecular Dynamics Investigation of the Structural and Dynamic Properties of the Ionic Liquid 1-n-Butyl-3-methylimidazolium Bis(trifluoromethanesulfonyl)imide. *J. Chem. Phys.* **2011**, *135*, 124507.